AIAA JOURNAL
Vol. 38, No. 9, September 2000

Implicit High-Order-Accurate-in-Space Algorithms for the Navier–Stokes Equations

John A. Ekaterinaris*
Nielsen Engineering and Research, Inc., Mountain View, California 94043-2212

High-order-accurate, alternating direction implicit schemes have been developed. These schemes can be used to obtain efficiently high-resolution numerical solutions of the compressible Euler and Navier–Stokes equations. Implicit solvers compatible with both centered and upwind schemes for the discretization of the convective terms are discussed. For centered space discretization of the convective fluxes, fourth-order spatial accuracy of the implicit operators is obtained at no additional computing cost by performing compact space differentiation. This implicit compact scheme, which requires block-tridiagonal matrix inversions, is used to obtain viscous and inviscid flow solutions in curvilinear coordinates. In addition, high-order-accurate-in-space implicit operators are obtained for diagonalized schemes, which require scalar matrix inversions. Both high-order algorithms improve convergence characteristics for subsonic and transonic flow compared to second-order-accurate-in-space implicit schemes. High-order-accurate-in-space implicit algorithms, compatible with upwind, high-resolution shock-capturing total variation diminishing schemes, are also developed. Third-order-accurate, upwind-biased, diagonalized algorithms were found to be as accurate and more efficient than the standard block-tridiagonal, implicit solvers.

I. Introduction

In recent years, there has been an increased interest in developing high-order, time-accurate methods[1–7] suitable for wave propagation, direct numerical simulation (DNS), and large eddy simulations (LES) of high-Reynolds-number, turbulent, compressible flows. High-resolution calculations with second-order-accurate-in-space implicit, finite difference and finite volume schemes often use iterative procedures to converge the solution within each implicit time step and rely on the high-order-accurate-in-space method, which is used for the discretization of the convective and viscous terms, to accurately represent the flow physics. For example, high-resolution simulations of wall-bounded flows in domains with stretched meshes[4,8] used factorized, implicit, iterative schemes. The implicit operators had a lower order of accuracy in space than the convective fluxes; therefore, additional subiterations within each physical time step were used during the computations to obtain time accuracy, remove factorization errors, and reduce errors caused by the low spatial order of accuracy of the implicit operators. As an alternative, the implicit schemes of Refs. 1, 3, and 6, which achieve high-order accuracy in space at no significant additional computing cost, can be used to perform these high-resolution calculations. Both unfactored and factorized implicit algorithms for nonlinear problems introduce linearization, and they are limited to second-order accuracy in time. High-order-accurate-in-space implicit operators, however, introduce smaller dispersion errors than second-order-accurate-in-space implicit methods. Therefore, they are more suitable not only for long time integration involved in LES but also for unsteady flow simulations in aerodynamics and other time-dependent flows. As a result, for unsteady problems, such as unsteady aerodynamics of rotor wakes, where space resolution is important, preservation of phase characteristics is required, and low numerical diffusion is critical. Significant advantages are expected from applications of high-order implicit methods.

Space discretization methods for hyperbolic-type equations are based on their semidiscrete form. This is the method of lines approach where we concentrate on the spatial discretization and retain the time variable continuous. Explicit time integration methods do not interfere with the spatial order of accuracy of the semidiscrete form. They are easier to analyze and can provide high-order-accurate time discretizations,[9] but they have numerical stability limitations. Implicit methods, on the other hand, introduce flux linearization and are usually second-order-accurate-in-time and more dispersive than high-order Runge–Kutta schemes, but they have no severe stability limitations. Second-order time accuracy is sufficient for simulations in unsteady aerodynamics and many wave propagation problems. A high-order of accuracy in space is employed as a more effective means of obtaining high resolution and good phase preservation characteristics at a reduced computing cost. It has been argued in Ref. 10 and references therein that accurate, steady-state and unsteady flow computational fluid dynamics (CFD) numerical simulations can be achieved with less computing effort by using globally high-order-accurate space discretizations. During the past few decades, many methods have been developed for the evaluation of the right-hand-side convective terms of the semidiscrete form with a high order of accuracy. Development and application of efficient and accurate implicit time integration schemes with these space discretization methods remain a challenge.[1,3,6]

Explicit and implicit time-marching methods are currently used in CFD for time integration of the compressible flow governing equations. Efficient explicit time integration methods require multigrid acceleration. These techniques have been applied in CFD to both steady-state[11] and time-accurate computations[12] with a second-order-accurate-in-space discretization. Implicit time marching has been performed with unfactored schemes[13] and with alternating direction implicit (ADI) methods, such as the Beam–Warming[14] algorithm. The Beam–Warming algorithm uses either central second-order-accurate differentiation in space with added artificial dissipation[15] or first-order-accurate upwinding.[8,16] The accuracy, efficiency, and convergence characteristics of implicit schemes can be improved by application of high-order discretization methods for the implicit operators. High-resolution schemes that provide a high order of accuracy in space for both the implicit and explicit operators, such as the fourth-order compact schemes recently presented by Abarbanel and Kumar[1] and Yee[3] and the implicit high-order-accurate-in-space schemes developed in this paper, can be used to improve the level of accuracy and solution at a given mesh size and to achieve faster convergence and high resolution.

The ability of high-order-accurate-in-space implicit schemes to compute efficiently and accurately time-dependent numerical solutions of linear and nonlinear problems was demonstrated in Ref. 6. In the present paper, high-order implicit schemes are extended to upwind methods; they are applied to curvilinear coordinates in general geometries; and they are used to obtain numerical solutions of problems relevant to aerodynamics. Specifically, in Sec. II we develop

Received 5 November 1998; presented as Paper 99-3257 at the AIAA 14th Computational Fluid Dynamics Conference, Norfolk, VA, 28 June–1 July 1999; revision received 4 February 2000; accepted for publication 28 February 2000.

*Senior Research Scientist, 526 Clyde Avenue; ekaterin@nearinc.com. Associate Fellow AIAA.

ADI, third- and fourth-order-accurate-in-space schemes for the Euler and Navier–Stokes equations. The resolution characteristics of discretization schemes are analyzed in Sec. III. The convergence characteristics of implicit schemes are illustrated for the case of the linear advection operator in Sec. IV. The improved convergence characteristics of the new high-order algorithms are demonstrated by performing comparisons with numerical solutions obtained from standard second-order-accurate-in-space implicit central-difference methods and upwind-biased implicit schemes. The new implicit schemes are easy to implement with existing implicit flow solvers (see Sec. V) and can be applied for time advancement of unsteady numerical simulations with large time steps and faster convergence to a steady state. Computed results are shown in Sec. VI, where examples of convergence tests for subsonic and transonic flow solutions are shown.

II. Implicit High-Order Schemes

A. Compact Space Discretization

A high order of accuracy in space can be used as an alternative to grid resolution[10] for aerodynamic flow calculations. High-resolution numerical simulations of complex time-dependent flows also require high-order-accurate-in-space discretizations because numerical approximations to the convective terms of the Euler and Navier–Stokes equations give rise to dispersive errors. For central-difference schemes, the dispersive errors are contributed mostly by the third derivative terms of the modified equation. Therefore, fourth-order spatially accurate algorithms not only achieve better accuracy but also yield less numerical diffusion by having better dispersive properties.

High-order-accurate spatial discretization of the right-hand side in semidiscrete form can be achieved by using small-stencil-size, centered, compact schemes.[17] These schemes do not require as wide a stencil as the explicit finite difference schemes but evaluate the spatial derivatives in a coupled fashion that implies solution of a tridiagonal or larger bandwidth system of linear equations. For example, the first derivative $\mathcal{F}'$ of a function $\mathcal{F}$ is computed with the fourth-order-accurate compact scheme for an equally spaced mesh with $\Delta x = 1$ as follows:

$$\mathcal{F}'_{j-1} + 4\mathcal{F}'_j + \mathcal{F}'_{j+1} = 3(\mathcal{F}_{j+1} - \mathcal{F}_{j-1}) \tag{1}$$

Evaluation of fourth-order-accurate first derivatives with Eq. (1) requires a scalar tridiagonal matrix inversion, which is obtained efficiently. A three-point stencil is involved in Eq. (1) as in the explicit second-order-accurate central differencing formula. Computing a first derivative with sixth-order accuracy[17] also requires inversion of a tridiagonal matrix but involves a larger, five-point stencil. Compact schemes can be applied for the entire computational domain using the one-sided formulas, which were presented by Carpenter et al.[18] for high-order compact schemes.

B. ADI Implicit Algorithms

Explicit schemes such as Runge–Kutta methods can yield a high order of accuracy in time, and they are the methods of choice for wave propagation problems.[9] An implicit algorithm, which provides a higher order of accuracy for time integration, is the fourth-order method for time integration of wave problems proposed by de Froutos and Sanz-Serna.[7] Each physical time step of this method is a succession of three implicit midpoint rule time integration steps. Application of this method to the nonlinear gasdynamic equations requires that each intermediate step be carried out with a suitable subiteration process until a certain convergence criterion is fulfilled, a requirement that makes the method very intensive computationally. Therefore, implicit time integration in CFD codes is performed with methods that use linearization of the convective terms as $\boldsymbol{F}^{n+1} = \boldsymbol{F}^n + (\partial \boldsymbol{F}/\partial \boldsymbol{Q})^n(\boldsymbol{Q}^{n+1} - \boldsymbol{Q}^n) + \mathcal{O}(\Delta t)^2 = \boldsymbol{F}^n + \boldsymbol{A}^n \Delta \boldsymbol{Q}^n + \mathcal{O}(\Delta t)^2$ and application of relaxation methods or approximate factorization. Flux linearization limits time accuracy to at most second order. Therefore, in the following sections an order of accuracy higher than second refers only to space discretizations. Factorized algorithms involve sweeps along each coordinate direction by implicit operators, such as $[\boldsymbol{I} + h\delta_\xi \boldsymbol{A}_{i,j}]$. Factorization errors can be reduced with the iterative form of the Beam–Warming algorithm,[8] which can be used for time-accurate computations with centered finite difference or finite volume methods.

C. Block-Tridiagonal High-Order Algorithm

The left-hand-side differentiations $\delta_\xi \boldsymbol{A}_{i,j}$ of the centered block-tridiagonal Beam–Warming algorithm[14] or its diagonalized form,[19] which requires scalar tridiagonal matrix inversions, are evaluated using second-order accurate central differences. Second-order implicit smoothing[15] is added for numerical stability. For upwind discretization of the right-hand side, a first-order-accurate upwinding of the flux-split[20] Jacobians as in Refs. 8 and 16 can be applied, and no implicit smoothing is needed for numerical stability. For both cases, along each line, only three-point stencils are involved, and a block-tridiagonal structure of the implicit operators is retained. Tridiagonal structure of the implicit factors yields a significant advantage in computing speed because inversion is performed efficiently. Recently, time-accurate, high-resolution computations were performed[4] where the right-hand-side derivatives were computed using high-order compact schemes, and the implicit operators were second-order accurate in space. Internal subiterations within each physical time step were used to drive the residuals to zero. The accuracy and efficiency of implicit algorithms, which are fourth-order accurate in space, were demonstrated in Ref. 6. Implicit time advancement with high-order-accurate-in-space operators helps to reduce the number of internal subiterations and improves convergence characteristics of the time integration. The block-tridiagonal structure of the implicit operators is retained by using compact differentiation formulas for the evaluation of the first-order derivatives. The computation of the derivatives in the implicit operators is carried out using the following fourth-order-accurate compact formula:

$$[\boldsymbol{A}(\Delta \boldsymbol{Q}^*)^p]'_{i-1,j} + 4[\boldsymbol{A}(\Delta \boldsymbol{Q}^*)^p]'_{i,j} + [\boldsymbol{A}(\Delta \boldsymbol{Q}^*)^p]'_{i+1,j} = 3\left\{[\boldsymbol{A}(\Delta \boldsymbol{Q}^*)^p]_{i+1,j} - [\boldsymbol{A}(\Delta \boldsymbol{Q}^*)^p]_{i-1,j}\right\} \tag{2}$$

In Eq. (2), $[\,]'$ denotes a spatial derivative that is evaluated with fourth-order accuracy and a three-point, compact stencil. Using Eq. (2) to evaluate the spatial derivatives, we obtain an algorithm that is fourth-order accurate in space and retains the block-tridiagonal matrix structure for the implicit operators because it only uses three-point stencils as follows:

$$\begin{aligned}
&(\boldsymbol{I} - 3h\boldsymbol{A}_{i-1,j})(\Delta \boldsymbol{Q}^*)^p_{i-1,j} + 4(\Delta \boldsymbol{Q}^*)^p_{i,j} \\
&\quad + (\boldsymbol{I} + 3h\boldsymbol{A}_{i+1,j})(\Delta \boldsymbol{Q}^*)^p_{i+1,j} = R^n_{i-1,j} + 4R^n_{i,j} + R^n_{i+1,j} = \boldsymbol{R}^n_4 \\
&(\boldsymbol{I} - 3h\boldsymbol{B}_{i,j-1})\Delta \boldsymbol{Q}^p_{i,j-1} + 4\Delta \boldsymbol{Q}^p_{i,j} + (\boldsymbol{I} + 3h\boldsymbol{B}_{i,j+1})\Delta \boldsymbol{Q}^p_{i,j+1} \\
&\quad = (\Delta \boldsymbol{Q}^*)^p_{i,j-1} + 4(\Delta \boldsymbol{Q}^*)^p_{i,j} + (\Delta \boldsymbol{Q}^*)^p_{i,j+1}
\end{aligned} \tag{3}$$

Spatial derivatives in the $R^n_{i,j}$ terms of Eq. (3) are computed with the fourth-order-accurate compact scheme of Eq. (1) to achieve a globally fourth-order-accurate-in-space algorithm. The temporal accuracy of the new algorithm given by Eq. (3) is at most second order as in the original Beam–Warming algorithm.[14] The fourth-order-accurate-in-space algorithm of Eq. (3) requires only a few more multiplications and additions compared to the original ADI algorithm of Ref. 14, where the left-hand-side operators are second-order accurate in space. Therefore, substantial savings in computer time can be obtained because it is not necessary to perform a large number of subiterations for high-order-accurate solutions. Numerical experiments have shown that, for time-accurate solutions, factorization and linearization errors are removed with only one additional subiteration.

D. Diagonalized High-Order Algorithm

Pulliam and Chaussee[19] diagonalized the block matrices as $\boldsymbol{A} = T_\xi \hat{\Lambda}_\xi T_\xi^{-1}$ and $\boldsymbol{B} = T_\eta \hat{\Lambda}_\eta T_\eta^{-1}$, where the $\hat{\Lambda}_\xi$ and $\hat{\Lambda}_\eta$ are diagonal eigenvalue matrices. The implicit operators of the diagonalized algorithm have the form $\{T_\xi[\boldsymbol{I} + h\delta_\xi \hat{\Lambda}_\xi]\}$. They are scalar tridiagonal and, during the ξ and η sweeps, the equations are solved in a decoupled fashion by independent scalar tridiagonal inversions. The latter were found to be from three to four times faster than the block tridiagonal algorithm inversions. Unfortunately, however, the diagonal

algorithm is only first-order accurate in time. Second-order time accuracy can be obtained if the diagonal algorithm is combined with a dual-time-step subiteration scheme. Time-marching schemes with internal subiterations were proposed for time-accurate solutions of incompressible flows with the artificial compressibility method by Merkle and Athavale[21] for explicit inner subiterations.

Evaluation of the first-order derivatives with standard, fourth-order-accurate, five-point-stencil, central-differencing formulas increases the bandwidth of the left-hand-side operators, and the diagonalized scalar matrices become pentadiagonal. The inversion of scalar pentadiagonal matrices is rather efficient, and the computational cost of the fourth-order-accurate diagonalized algorithm is still reasonable. For a higher order of accuracy, however, the computing cost increases rapidly. Compact high-order-accurate-in-space implicit operators as in Eq. (2) can be constructed to obtain fourth- or sixth-order accuracy in space by inverting scalar tridiagonal or pentadiagonal matrices, respectively. The fourth-order compact differentiation formula of Eq. (2), with Λ replacing $\boldsymbol{A}$, applied for the evaluation of the derivatives in the diagonalized algorithm, yields the following one-dimensional diagonalized operators:

$$
\begin{aligned}
&[\boldsymbol{I} - 3h(\hat{\Lambda}_\xi)_{i-1,j}]\Delta(\boldsymbol{Q}^*)^n_{i-1,j} + 4\Delta(\boldsymbol{Q}^*)^n_{i,j} \\
&\quad + [\boldsymbol{I} + 3h(\hat{\Lambda}_\xi)_{i+1,j}]\Delta(\boldsymbol{Q}^*)^n_{i+1,j} \\
&\quad = R^n_{i-1,j} + 4R^n_{i,j} + R^n_{i+1,j} = \boldsymbol{R}^n_4 \\
&[\boldsymbol{I} - 3h(\hat{\Lambda}_\eta)_{i,j-1}](\Delta\boldsymbol{Q})^n_{i,j-1} + 4(\Delta\boldsymbol{Q})^n_{i,j} \\
&\quad + [\boldsymbol{I} + 3h(\hat{\Lambda}_\eta)_{i,j+1}](\Delta\mathbf{Q})^n_{i,j+1} \\
&\quad = (\Delta\boldsymbol{Q}^*)^n_{i,j-1} + 4(\Delta\boldsymbol{Q}^*)^n_{i,j} + (\Delta\boldsymbol{Q}^*)^n_{i,j+1}
\end{aligned}
\tag{4}
$$

In this equation, the scalar tridiagonal structure of the implicit operators is retained and fourth-order accuracy in space is obtained. The algorithm of Eq. (4) is only first-order accurate in time and suitable for steady-state calculations. Second-order accuracy in time can be obtained by using dual time stepping. Use of the sixth-order-accurate compact differencing for the evaluation of the derivatives of the left-hand side yields a sixth-order-accurate implicit algorithm.[6] Evaluation of the derivative with the sixth-order-accurate-in-space compact scheme,[17] even though it requires inversion of tridiagonal matrices, involves a five-point stencil. Therefore, evaluation of the spatial derivatives in the implicit operators with a formula similar to Eq. (2), which yields a sixth-order-accurate-in-space implicit scheme, involves a five-point stencil and requires inversion of pentadiagonal matrices.[6] For the sixth-order-accurate scheme, either the order of accuracy on the computational boundaries is dropped to fourth order or the boundary schemes of Ref. 18 are used.

E. Upwind Algorithms

High-order, upwind shock-capturing schemes were proven effective for the numerical solution of subsonic, transonic, and high-speed supersonic compressible flows. High-order-accurate upwind discretization of the convective fluxes is performed with total variation diminishing (TVD) and essentially nonoscillatory schemes for high-resolution numerical simulations of flows that contain discontinuities. Highly stretched meshes are needed for resolution of the near wall flow gradients of large-Reynolds-number viscous flows, and implicit schemes capable of marching the solution with large time steps are usually employed. The evaluation of exact Jacobians for upwind schemes is costly. Implicit forms of these upwind schemes either evaluate the approximate Jacobians or use Steger–Warming flux vector splitting.[20] To retain the block-tridiagonal structure of the implicit operators, a first-order-accurate-in-space upwinding is applied. Numerical solutions obtained with algorithms that use the Steger–Warming splitting of the flux Jacobian were found to be accurate for both steady and time-dependent computations.[16]

Implicit methods for upwind shock-capturing schemes based on the Beam–Warming algorithm were used in Refs. 8 and 16, where the flux vector Jacobians $\widehat{A^{\pm}}_{i,j}$ and $\widehat{B^{\pm}}_{i,j}$ were evaluated approximately with flux vector splitting.[20] Evaluation of the flux-split Jacobians consumes a large portion of the computing time needed to advance the solution by one time step implicitly. As an alternative, the implicit diagonalized algorithm[19] with subiterations within each time step may be used. For convergence to a steady state, the first-order-accurate-in-time algorithm[19] can be used. For time-accurate computations, the second-order-accurate-in-time, dual-time-stepping algorithm is required. An upwind, diagonalized algorithm, where the space derivatives $\delta_\xi\hat{\Lambda}_\xi$ and $\delta_\eta\hat{\Lambda}_\eta$ in the implicit, one-dimensional operators are evaluated with forward and backward differencing formulas according to the sign of the eigenvalues, is shown next. The viscous Jacobian $\hat{M}_{i,j}$ does not diagonalize simultaneously with the inviscid flux Jacobians, and for viscous flow solutions the spectral radius of $\hat{M}$ can be added for numerical stability.

1. *Upwind-Biased Diagonal Algorithm*

The implicit operator matrices retain tridiagonal structure when the derivatives are evaluated using first-order upwinding formulas as $\delta_\xi\lambda = \Delta^f\lambda = \lambda_i - \lambda_{i-1}$ for $\lambda \geq 0$, and $\delta_\xi\lambda = \nabla^b\lambda = \lambda_i - \lambda_{i+1}$ for $\lambda < 0$. First-order upwinding is too diffusive, and third-order accuracy in space can be obtained at the expense of performing scalar tridiagonal matrix inversion when the spatial derivatives are evaluated with the following upwind biased formulas:

$$
\begin{aligned}
\delta_\xi\lambda = \Delta^f\lambda &= \tfrac{1}{6}(2\lambda_{i+1} + 3\lambda_i - 6\lambda_{i-1} + \lambda_{i-2}) \qquad \lambda \geq 0 \\
\delta_\xi\lambda = \nabla^b\lambda &= \tfrac{1}{6}(-2\lambda_{i-1} - 3\lambda_i + 6\lambda_{i+1} - \lambda_{i+2}) \qquad \lambda < 0
\end{aligned}
\tag{5}
$$

The upwind space differencing is inherently dissipative; therefore, the addition of implicit smoothing terms suggested in Ref. 15, which are necessary for the central difference algorithms, is not required. Addition of a small amount of implicit dissipation, however, enhances diagonal dominance, yields better stability, and allows viscous flow solutions to advance with large time steps. The accuracy of the computed steady-state solutions is unaffected by the implicit smoothing.

2. *Compact, Upwind Diagonal Algorithms*

High-order accuracy in space can also be obtained by compact, upwind space differentiation as follows:

$$
\begin{aligned}
D^b f &= f'_{j-1} - 5f'_j + f'_{j+1} = -\tfrac{3}{2}[3f_j - 4f_{j-1} + f_{j-2}] \\
D^f f &= f'_{j-1} - 5f'_j + f'_{j+1} = \tfrac{3}{2}[3f_j - 4f_{j+1} + f_{j+2}]
\end{aligned}
\tag{6}
$$

Either a backward or forward compact differentiation formula from Eq. (6) is used, according to the sign of the eigenvalues. When we use D^f for positive λ and D^b for negative λ, the following compact implicit scheme is obtained for the i sweep along ξ direction:

$$
\begin{aligned}
&\left[-\tfrac{3}{2}(\Lambda_\xi)_{i-2}\right](\Delta\boldsymbol{Q}^*)^p_{i-2,j} + [\boldsymbol{I} + 6(\Lambda_\xi)_{i-1}](\Delta\boldsymbol{Q}^*)^p_{i-1,j} \\
&\quad + \left[-5\boldsymbol{I} - \tfrac{9}{2}(\Lambda_\xi)_i\right](\Delta\boldsymbol{Q}^*)^p_{i,j} + [\boldsymbol{I}](\Delta\boldsymbol{Q}^*)^p_{i+1,j} \\
&\quad = R^n_{i-1,j} - 5R^n_{i,j} + R^n_{i+1,j} = \boldsymbol{R}^n_3
\end{aligned}
\tag{7}
$$

for positive eigenvalues with an analogous equation for negative eigenvalues. The compact diagonalized algorithm of Eq. (7) and the diagonalized algorithm obtained by applying the upwind space discretization for the evaluation of δ_ξ and δ_η by the use of Eq. (5) provide a higher order of accuracy in space, but they both require matrix inversion of a bandwidth larger than three. The inversion of these scalar matrices is obtained with standard lower-upper decomposition methods.

3. *Compact Block-Tridiagonal Algorithm*

Upwind compact schemes with centered grid stencils were developed by Adams and Shariff[2] and Zhong[5] for direct numerical simulations of compressible turbulent flows. The order of accuracy of the centered, upwind, compact, finite difference schemes of Ref. 5 is lower by one order than the maximum order of accuracy that analogous central-difference compact schemes can achieve. For example, the general form of a third-order upwind scheme is

$$A_{i-1}f'_{i-1} + A_i f'_i + A_{i+1}f'_{i+1} = \pm(B_{i-1}f_{i-1} + B_i f_i + B_{i+1}f_{i+1}) \quad (8)$$

where the + is for positive speeds and the − corresponds to negative wave speeds or eigenvalues. The coefficients of Eq. (8) are $A_{i\pm1} = 15(\kappa \mp 3)$, $A_i = 60\kappa$ and $B_{i\pm1} = -15(\kappa \mp 3)$, $B_i = 60\kappa$. For $\kappa = 0$ we obtain the standard, fourth-order-accurate, central, compact, finite difference scheme of Eq. (1), and for $\kappa > 0$, Eq. (8) yields upwind biased schemes. Different resolution and numerical diffusion is obtained by varying κ. The suggested value is $\kappa = 0.4$ (Ref. 5), which yields a resolution in wave space comparable to the resolution obtained by the fourth-order-accurate compact scheme of Eq. (1) and very little dissipation compared to other upwind schemes. A block-tridiagonal implicit scheme can be obtained with compact differentiation for the evaluation of flux-split matrix differences $\nabla^b_\xi \widehat{A^+}_{i,j}$ and $\Delta^f_\xi \widehat{A^-}_{i,j}$ using Eq. (8). The resulting third-order-accurate, upwind block-tridiagonal implicit scheme for the ξ sweep along the i direction, which involves the flux Jacobian $\widehat{A^\pm}_{i,j}$, is as follows:

$$\left(5\boldsymbol{I} \mp 14h\widehat{A^\pm}_{i-1,j}\right)(\Delta\boldsymbol{Q}^*)^p_{i-1,j} + \left(16\boldsymbol{I} \pm 4h\widehat{A^\pm}_{i,j}\right)(\Delta\boldsymbol{Q}^*)^p_{i,j} + \left(3\boldsymbol{I} \pm 10h\widehat{A^\pm}_{i+1,j}\right)(\Delta\boldsymbol{Q}^*)^p_{i+1,j} = 5\boldsymbol{R}^n_{i-1,j} + 16\boldsymbol{R}^n_{i,j} + 3\boldsymbol{R}^n_{i+1,j} = \boldsymbol{R}^n_{3C} \quad (9)$$

The diagonalized third-order implicit scheme, which requires scalar tridiagonal matrix inversions, is readily obtained by Eq. (9) by substituting $\widehat{A^\pm}_{i,j}$ with $\Lambda^\pm_{i,j}$.

III. Spatial Resolution

In this section we show the resolving ability of the discretization schemes used for the evaluation of the first derivative of the one-dimensional implicit operators. The resolving ability of each scheme is defined in the Fourier space in terms of a modified wave number. This method, which was introduced in Refs. 17 and 22, provides a convenient means of quantifying the error associated with finite difference schemes. It considers that the solution is represented by a test sinusoidal function $f_j = e^{ik\Delta x_j}$, where Δx_j is the grid spacing and $\boldsymbol{k}$ is the wave number. The exact value of the test solution first derivative f'_j is $f'_j = i\boldsymbol{k}f_j$, and the derivative computed with finite differences will be $i\hat{\boldsymbol{k}}f_j$, where $\hat{\boldsymbol{k}}$ is the modified wave number. The form of $\hat{\boldsymbol{k}}$ depends on the difference formula that is used for the evaluation of the derivative. The difference between $\boldsymbol{k}$ and $\hat{\boldsymbol{k}}$ is a measure of the scheme's resolving ability.

The modified wave numbers are obtained when we use the relations such as $f'_{j\pm1} = f'_j e^{\pm ik}$ for the space derivatives. The modified wave number of the compact scheme of Eq. (1), for example, is obtained by $f'_j[e^{ik} + 4 + e^{-ik}] = 3f_j(e^{ik} - e^{-ik})$ or $\hat{\boldsymbol{k}} = 3\sin\boldsymbol{k}/(2 + \cos\boldsymbol{k})$. The modified wave numbers, $\hat{\boldsymbol{k}}^c$, for various central-differencing schemes used for the evaluation of the first derivative are as follows: second-order-accurate explicit evaluation, $\hat{\boldsymbol{k}}^c_{2e} = \sin\boldsymbol{k}$; fourth-order-accurate explicit evaluation, $\hat{\boldsymbol{k}}^c_{4e} = (8\sin\boldsymbol{k} - \sin 2\boldsymbol{k})/6$; and fourth-order-accurate compact evaluation, $\hat{\boldsymbol{k}}^c_{4c} = 3\sin\boldsymbol{k}/(2 + \cos\boldsymbol{k})$. Upwind difference schemes are inherently dissipative because they introduce numerical smoothing. As a result, their modified wave number, $\hat{\boldsymbol{k}}^u$, has an imaginary part that is proportional to this smoothing and is a measure of the dispersive properties of these schemes. The modified wave numbers of the upwind schemes, $\hat{\boldsymbol{k}}^u$, are as follows: first-order-accurate explicit evaluation, $\hat{\boldsymbol{k}}^u_{1e} = \sin\boldsymbol{k} \pm i(1 - \cos\boldsymbol{k})$; third-order-accurate explicit evaluation, $\hat{\boldsymbol{k}}^u_{3e} = [(8\sin\boldsymbol{k} - \sin 2\boldsymbol{k}) \pm i(4\cos\boldsymbol{k} - \cos 2\boldsymbol{k} - 3)]/6$; and third-order-accurate compact evaluation, $\hat{\boldsymbol{k}}^u_{2c} = 3[(4\sin\boldsymbol{k} - \sin 2\boldsymbol{k}) \pm i(4\cos\boldsymbol{k} - \cos 2\boldsymbol{k} - 3)]/(10 - 4\cos\boldsymbol{k})$. In these equations, the ± sign refers to the forward and backward difference operators, respectively. Note that the first-order upwind formula and the second-order central-difference formula have the same resolving ability apart from the numerical diffusion term that is introduced by the imaginary part. The implicit smoothing term added for numerical stability of central-difference methods has the form $\epsilon_{\text{impl}}\rho_j(D_{j+1} - 2D_j + D_{j-1})$, where ϵ_{impl} is a coefficient and ρ_j is the spectral radius of the flux Jacobian matrix. The modified wave number of this term is proportional to $(1 - \cos\boldsymbol{k})$, which is the imaginary part of the first-order-accurate upwind formula $\hat{\boldsymbol{k}}^u_{1e}$. Similarly, the real part of the third-order, upwind-biased scheme is equal to the modified wave number of the fourth-order, central-differencing scheme.

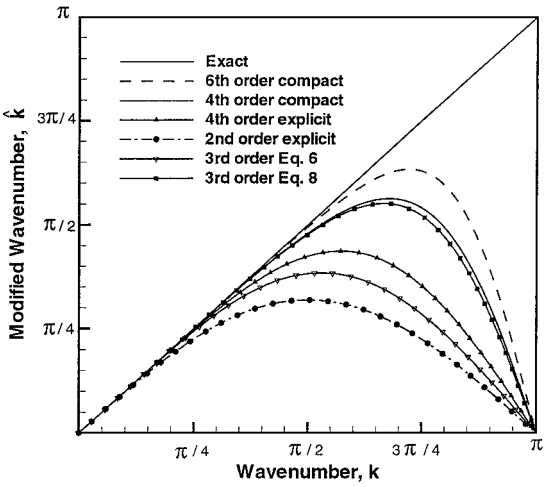

Fig. 1 Resolving ability of centered and upwind differencing schemes.

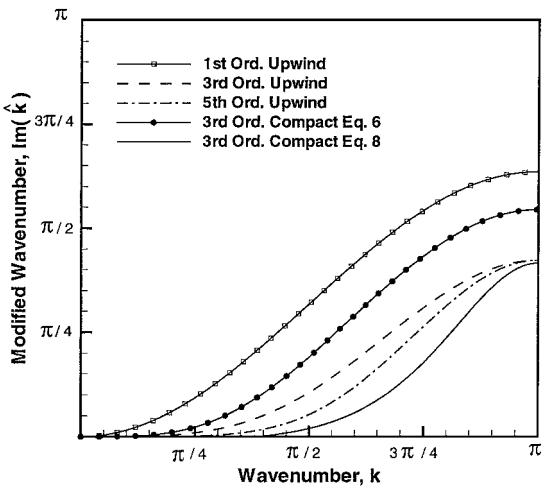

Fig. 2 Imaginary part of the modified wave number of upwind differencing schemes.

Figure 1 shows the error of various schemes for the range of wave numbers from 0 to π. The real part of $\hat{\boldsymbol{k}}^u$ is plotted for the upwind schemes. The sixth- and fourth-order, central, compact schemes have the best resolution in the high wave numbers compared to all other schemes. The third-order compact differencing scheme has a lower resolving ability than the third-order, upwind-biased explicit differencing formula, which has the same real part as the modified wave number of the fourth-order centered scheme that is symmetric and has no imaginary part. The imaginary part of the upwind schemes is plotted in Fig. 2. The first-order scheme is very diffusive. The compact, centered stencil scheme introduces lower diffusion for high wave numbers, a feature that makes it more suitable for high-resolution computations. For comparison, the imaginary part of the fifth-order upwind differencing formula $f'_j = [f_{j+3} - 6f_{j+2} + 18f_{j+1} - 10f_j - 3f_{j-1}]/12$, which has modified wave number $\hat{\boldsymbol{k}} = [(21\sin\boldsymbol{k} - 6\sin 2\boldsymbol{k} + \sin 3\boldsymbol{k}) \pm (10 - 15\cos\boldsymbol{k} + 6\cos 2\boldsymbol{k} - \cos 3\boldsymbol{k})]/12$, is plotted in Fig. 2 to demonstrate the superior performance of the compact operator.

IV. Stability and Convergence

It is shown in Ref. 6 that the fourth-order compact scheme is unconditionally stable for two-dimensional linear hyperbolic problems, such as the two-dimensional wave equation. To further explore the properties of the proposed high-order-accurate implicit time-marching methods, we perform an eigenspectrum analysis of the

schemes for the simple case of the advection operator. It was pointed out in Ref. 22 that the simple advection equation $u_t + cu_x = 0$, where c is a constant wave speed, is a good model for the description and investigation of the properties of numerical approximations of hyperbolic systems.

The fourth-order-accurate, implicit compact scheme of Eq. (3) or (4) applied to the scalar equation reduces to the following form:

$$(1 - 3\Delta t)\Delta U^n_{i-1} + 4U^n_i + (1 + 3\Delta t)\Delta U^n_{i+1} = -\Delta t c \boldsymbol{R}^n(U) \quad (10)$$

where U^n_i is the numerical approximation to u, $\Delta U^n_i = U^{n+1}_i - U^n_i$, and $\boldsymbol{R}^n(U)$ is the discrete form of the residual that is computed with a fourth- or higher-order compact scheme. The asymptotic stability of numerical methods for the equation $u_t + cu_x = 0$ is determined from the semidiscrete form (a set of equations $du_i/dt = c\mathcal{M}_{i,j}u_j$, where $u'_j = \mathcal{M}_j u_j$) by inspection of the eigenvalue spectrum of the matrix $\mathcal{M}$ resulting from the spatial discretization of the derivative u_x with finite differences. Similarly, the asymptotic stability of the implicit numerical scheme given by Eq. (10) is determined by $\Delta U_i = -(c\Delta t)\mathcal{D}U^n_i$ and the eigenvalues of the matrix $\mathcal{D}$, which is defined by

$$\frac{du}{dt} \approx \frac{\Delta u_i}{\Delta t} = -c(A^{-1}B)U^n_i = -c\mathcal{D}U^n_i \quad (11)$$

where A is the implicit tridiagonal operator matrix for the fourth-order compact scheme. The diagonal elements of this matrix are $a_{ii} = 4$ and the upper and lower off-diagonal elements are given by $\mathcal{T}^{\pm} = 1 \pm 3\Delta t$, respectively. The matrix B depends on the method used for the discretization of u_x. The numerical scheme for $u_t + cu_x = 0$ is unconditionally stable when the eigenvalues of $\mathcal{D}$ are all negative. For periodic boundary conditions and equally spaced mesh, the convergence rate is independent of the number of intervals. The convergence rate is affected, however, by the discretization method and increases with increasing Δt. The eigenvalue spectrum of $\mathcal{D}$ in Eq. (11) was computed for different values of Δt and number of points. It was shown that the shape of the eigenspectrum is not affected by the number of points used for the discretization.[23] For clarity, however, the eigenspectra of Fig. 3 are drawn with 25 points. Larger time steps result in more rapid convergence. In Fig. 3, the eigenspectrum obtained by the implicit compact scheme of Eq. (10), for $\Delta t = 0.1$, is compared with the eigenspectra obtained by the application of the second-order-accurate-in-space Beam–Warming algorithm.[14] Figure 3 is a plot of the eigenspectrum of the implicit algorithm that uses fourth-order explicit formulas for the evaluation of δ_x in both the residual term $\boldsymbol{R}$ and the implicit operator. This scheme requires a pentadiagonal matrix inversion. Faster convergence is achieved with the compact implicit tridiagonal scheme. For the linear case convergence is equivalent to stability. For nonlinear systems, the Lax–Wendroff theorem[24] guarantees that the solution to the conservative scheme, of the form

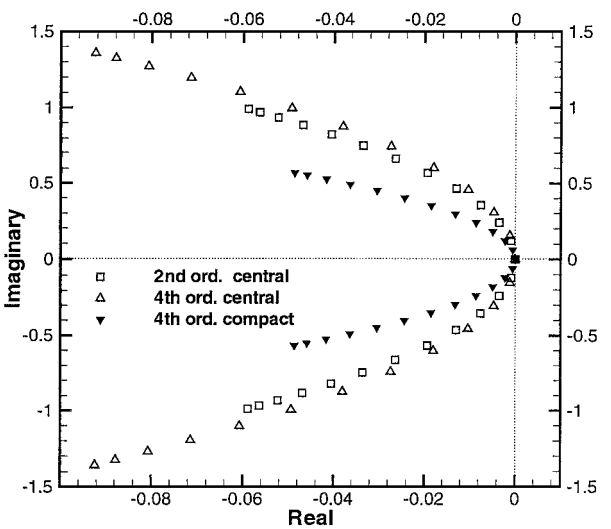

Fig. 3 Eigenspectrum comparison for different implicit methods.

$du/dt = -[f(u_{i+1/2}) - f(u_{i-1/2})]$, if it converges, will converge to a weak solution. The convergence of numerical schemes in multidimensional cases and nonlinear numerical fluxes $f(u)$, which are of interest to practical applications, must be demonstrated with numerical tests. It will be shown in the results section that these findings for the simple advection operator, $u_t + cu_x = 0$, carry over to the more complex nonlinear case of the numerical solutions of the Euler and Navier–Stokes equations in curvilinear meshes.

V. Implementation

High-order-accurate-in-space numerical solutions require smooth meshes. For consistency, the metric terms, ξ_x, ξ_y, etc., are evaluated with the same order of accuracy and method as the one used for the discretization of the convective terms. For example, in solutions that were computed with the fourth-order-accurate-in-space implicit scheme of Eq. (3), both the convective and metric terms are evaluated with the fourth-order, compact differencing formula of Eq. (1). The boundary closures of Ref. 18 were used to compute the metrics at the boundaries of the domain. It was found that excessive grid stretching and nonsmooth grids yield numerical oscillations, degrade convergence, and result in loss of accuracy. For the upwind methods, the order of accuracy of the metrics is chosen according to the resolving ability of the scheme. For the first- and third-order-accurate-in-space schemes, the metrics are computed with central differences, whereas for the third-order scheme of Eq. (7), fourth-order-accurate metrics are needed.

A. Boundary Treatment

The fourth-order-accurate-in-space, implicit algorithms of Eqs. (3) and (4) can be applied in the computational domain for mesh points between $i = 2$, $i = I_{\max} - 1$ and $j = 2$, $j = J_{\max} - 1$, because the modified right-hand-side residual term $\boldsymbol{R}^n_{i,j_4} = R^n_{i-1,j} + 4R^n_{i,j} + R^n_{i+1,j}$ of Eq. (3) is evaluated with a three-point stencil. During the I sweep, the values of $R_{1,j}$ and $R_{I\max,j}$ in $\boldsymbol{R}^n_4$ are needed for the inversion. The residual terms at the boundary points can be computed with the one-sided compact operators developed by Carpenter et al.[18] At the open boundaries of the domain we can also supply boundary conditions in differential form (see, for example, Ref. 25). The results presented in the next section were obtained using simple explicit boundary conditions. For an explicit update of the computational domain boundaries, the residual term $R_{i,j}$ is zero at the edges of the domain ($i = 1$ and $i = I_{\max}$ for all j and for $j = 1$ and $j = J_{\max}$ for all i). Values of the intermediate term $(\Delta\boldsymbol{Q}^*)_{i,j}$ at $j = 1$ and $j = J_{\max}$ can be obtained during the i sweep, which is carried out for $i = 2$, $I_{\max} - 1$ and for all j, by setting $R_{1,j} = R_{I\max,j} = 0$ at $j = 1$ and $J_{\max}$ in the modified residual term $\boldsymbol{R}^n_4$. During the j sweep, the terms $(\Delta\boldsymbol{Q}^*)_{i,1}$ and $(\Delta\boldsymbol{Q}^*)_{i,J\max}$ needed for the evaluation of $(\Delta\boldsymbol{Q}^*)_4 = (\Delta\boldsymbol{Q}^*)_{i,j-1} + 4(\Delta\boldsymbol{Q}^*)_{i,j} + (\Delta\boldsymbol{Q}^*)_{i,j+1}$ are available. This explicit update of the boundary points is straightforward to implement and was found to be stable for the implicit compact solvers. The implicit higher-order-accurate compact solvers require only a moderate (approximately 10%) increase in computing cost because they require a larger operation count for the formation of the coefficient matrices.

B. Filtering and Numerical Smoothing

Numerical solutions of nonlinear problems require damping of high-frequency modes that are not resolved by the numerical mesh. This is accomplished either by using numerical dissipation or by applying spatial filtering to the solution vector. Consistent with the compact space discretization are the compact filtering schemes suggested in Refs. 4 and 17. Implicit seven-point filter formulas were suggested in Ref. 17, where a sixth-order pentadiagonal and a fourth-order tridiagonal spatial filter were shown. Tridiagonal 8- and 10-order filters were used in Ref. 4. These implicit filters obtain the filtered values of the conserved variables $\hat{q}$ from the unfiltered values q by solving

$$a_f\hat{q}_{i-1} + \hat{q}_i + a_f\hat{q}_{i+1} = \sum_{n=0}^{N} \frac{a_n}{2}(q_{i+n} + q_{i-n}) \quad (12)$$

This is an Nth-order filter with a $2N + 1$ point stencil. The coefficients for the tridiagonal 8th-order and 10th-order filters can be found in Ref. 4. Filtering is applied sequentially one direction at a time, on the conserved variables, after each subiteration for implicit time integration. Implicit second-order filters can be obtained from Eq. (12). These filters require three-point stencils, and for large values of the parameter a_f have good spectral characteristics,[4] not filtering out wave numbers less than $\pi/2$. Therefore, at the computational domain boundaries, instead of using one-sided, high-order explicit filters, the filter order is reduced and improved low dissipation spectral characteristics are obtained by increasing the value of the parameter a_f as is suggested in Ref. 4. A detailed investigation of the effect of numerical filtering has been presented in Ref. 4.

Second-order-accurate solutions were obtained with the standard explicit dissipation given in Ref. 15. Solutions that include discontinuities and evaluate the convective derivatives with fourth-order-accurate central differences use a blending of second- and sixth-order-explicit dissipation terms. The second-order terms are active only in the vicinity of discontinuities. The following sixth-order operator is always active for numerical stability; $\mathcal{D}^e_{i,j} = \nabla_x \hat{\rho}(-\epsilon_{\text{expl}} \Delta_x \nabla_x \Delta_x \nabla_x \Delta_x q_{i,j})$, where $\hat{\rho} = (\rho_{i+1,j} + \rho_{i,j})$, $\rho_{i,j}$ is the spectral radius of $\boldsymbol{A}$, and ϵ_{expl} is chosen, as suggested in Ref. 15.

VI. Results

The second-order-accurate-in-time, high-order-accurate-in-space implicit time-marching schemes of Eqs. (3–5) presented in the preceding sections are tested for inviscid and viscous flow numerical solutions over a NACA-0012 airfoil at subsonic and transonic speeds. High-order-accurate-in-space numerical solutions with sparser grids were in agreement with results obtained from standard second-order-accurate methods and finer grids. The accuracy of second-order-in-space implicit methods is well established, and detailed comparisons are not shown. In Refs. 4 and 6 it was demonstrated that use of high-order compact schemes for the discretization of the right-hand-side convective terms can yield significant savings in the total number of grid points required for an accurate solution. It was also shown that high-order-accurate-in-space methods are more effective in convecting vorticity to long distances without distortion.[4,6] The physics of the problem are governed by the accuracy and the method that is used to evaluate the right-hand-side terms. Increasing the number of subiterations within each physical time step for time-accurate computations or the total number of iterations for steady-state solutions can yield highly accurate solutions, provided that the computations are well resolved either by high grid resolution or a high order of accuracy and the numerical scheme converges. The objective of this section is to demonstrate that the new high-order-accurate-in-space implicit schemes converge at least as fast as their standard lower-order-accurate counterparts. Illustrative examples of this section demonstrate the convergence rates of the proposed implicit schemes in the same sequence in which they were presented in Sec. III.

The fourth-order-accurate implicit scheme of Eq. (3) is tested for viscous and inviscid flow solutions. Inviscid flow solutions over the NACA-0012 airfoil are obtained for all cases with the same time step on a 201×41 point grid at an angle of incidence $\alpha = 5$ deg. The surface pressure coefficient obtained from steady-state computations with the second-order-accurate-in-space Beam–Warming algorithm,[14] the compact fourth-order-accurate-in-space implicit scheme of Eq. (3), the diagonalized scheme,[19] and the compact fourth-order-accurate-in-space diagonalized scheme of Eq. (4) are in agreement within plotting accuracy. The computed surface pressure coefficient distribution (shown in Ref. 23) was in good agreement with the experiment.[26] It was possible to obtain the same level of accuracy achieved with computations on the 201×41 point grid using a 151×31 point grid with the high-order scheme.

The following comparisons demonstrate that the new high-order schemes, in addition to accuracy, yield a faster convergence compared to lower-order methods. The rate of convergence of the compact scheme, although faster than the second-order-accurate-in-space schemes (Fig. 4), still remains algebraic. Therefore, if convergence is like $1/(\mathcal{N}^\gamma)$ for all implicit schemes, the exponent γ is larger for the compact, fourth-order-accurate-in-space scheme. The convergence rates of Fig. 4 for numerical solutions of inviscid flow that are obtained with block-tridiagonal algorithms are measured by the maximum, L_2 norm of the density residual. The solutions obtained with the second-order-accurate-in-space tridiagonal algorithm[14] for implicit time marching and a different order of accuracy on the right-hand side show the same rate of convergence after the initial transients are removed, for example, after $T \approx 1$. The solution obtained with the fourth-order-accurate-in-space compact implicit scheme for time marching, and use of fourth-order-accurate-in-space compact differentiation for the right-hand-side convective terms, shows a convergence rate approximately an order of magnitude faster than the solutions obtained with second-order-accurate-in-space implicit scheme. Fourth-order-accurate subsonic flow solutions were obtained using implicit filtering and the high-order numerical dissipation. The accuracy and convergence of the numerical solution was the same in both cases.

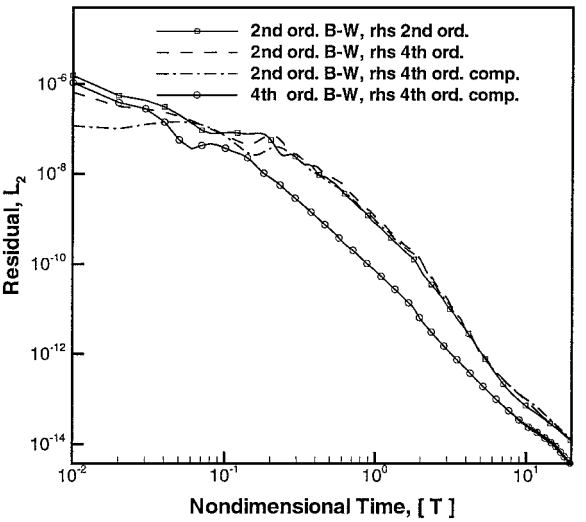

Fig. 4 Convergence of the block-tridiagonal implicit algorithms for inviscid flow solutions at subsonic speeds; $M = 0.3$, $\alpha = 5$ deg, inviscid.

The fourth-order-accurate-in-space, ADI algorithm of Eq. (3) is also used for the computation of viscous flow solutions over a NACA-0012 airfoil. A 201×91 point grid is used for viscous flow solutions, which are obtained for $Re = 5.0 \times 10^6$ as fully turbulent using the algebraic eddy viscosity model of Ref. 27. The thin-layer approximation of the viscous terms[27] is used. The viscous terms are added to the implicit part for the j sweep along the normal to wall η direction. The inviscid and viscous flux matrices do not diagonalize simultaneously. Therefore, the diagonalized algorithm cannot include the viscous fluxes. Viscous flow solutions with the diagonalized algorithm can be obtained, probably with a smaller time step, by adding the spectral radius of the viscous matrix to the j sweep implicit operator. Fourth-order accuracy in space for the viscous terms can be obtained either by computing the second-order derivative using explicit or compact differencing formulas or by evaluating the first-order derivative twice. Recently, in Ref. 28, a class of new compact high-resolution schemes was introduced. These schemes compute simultaneously the first and second derivative and achieve better resolution in wave space than the compact schemes of Ref. 17 for the same order of accuracy and stencil width.

A comparison of convergence rates for viscous flow solutions obtained by block-tridiagonal algorithms is shown in Fig. 5. The solutions computed with second-order spatial accuracy on the implicit operator have the same asymptotic convergence, whereas the fourth-order implicit compact scheme has faster convergence for viscous highly stretched meshes. Convergence rates for transonic inviscid flow solutions over the NACA-0012 airfoil are shown in Fig. 6. These solutions were obtained with the explicit smoothing. The same trends observed for subsonic flow carry over to flow solutions with discontinuities. It is illustrative to show the convergence rate of transonic flow solutions with the maximum residual. For these cases the maximum residual occurs at the shock, and as the

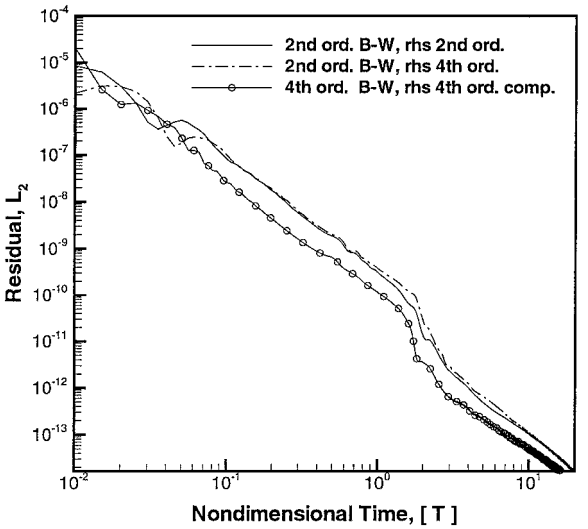

Fig. 5 Convergence of the block-tridiagonal implicit algorithms for viscous flow solutions at subsonic speeds; $M = 0.3$, $\alpha = 5$ deg, and $Re_c = 5.0 \times 10.^6$

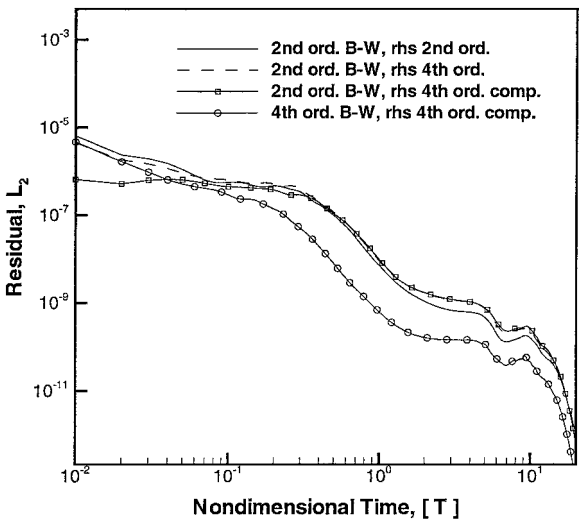

Fig. 6 Convergence of the block-tridiagonal implicit algorithms for inviscid flow solutions at transonic speeds; $M = 0.8$, $\alpha = 0.1$ deg, inviscid.

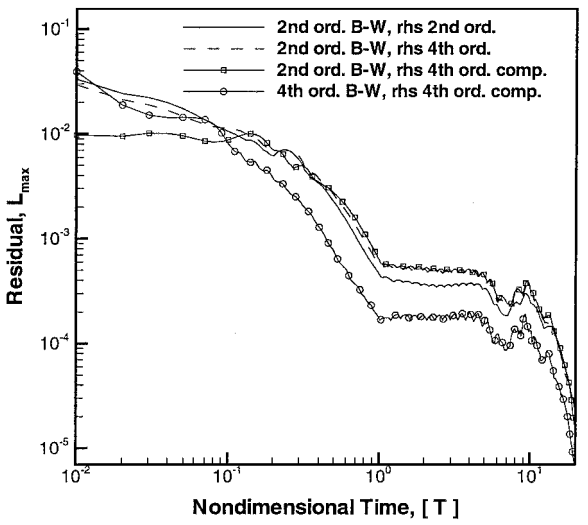

Fig. 7 Maximum residual of inviscid flow solutions convergence at transonic speeds; $M = 0.8$, $\alpha = 0.1$ deg, inviscid.

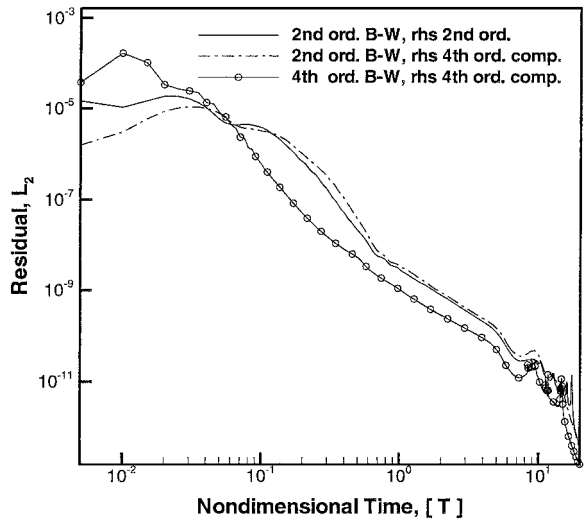

Fig. 8 Convergence of the block-tridiagonal implicit algorithms for viscous flow at transonic speeds; $M = 0.8$, $\alpha = 0.1$ deg, and $Re_c = 5.0 \times 10.^6$

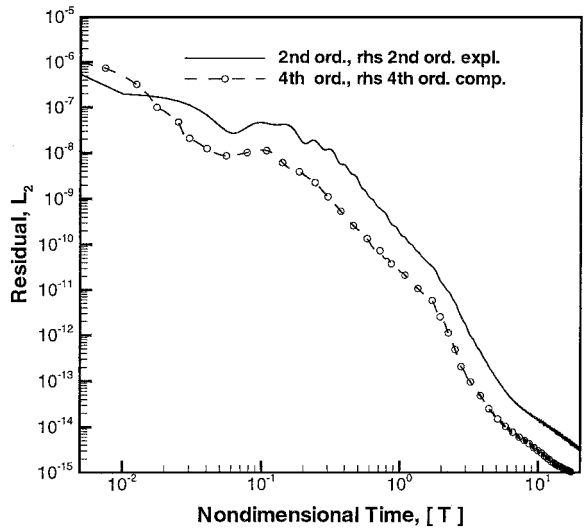

Fig. 9 Convergence rate of the diagonalized implicit algorithm for inviscid flow solutions at subsonic speeds; $M = 0.3$, $\alpha = 5$ deg, inviscid.

shock moves until it stabilizes, these residuals do not reduce. After the shock attains a stationary position, the solution further converges down to the truncation error. A plot of convergence based on the maximum norm for transonic flow solutions is shown in Fig. 7. Convergence rates for viscous flow solutions of transonic flow are shown in Fig. 8.

Inviscid flow solutions with the centered diagonalized algorithm of Eq. (4) are obtained for airfoil flows at subsonic and transonic speeds. The convergence rates obtained for subsonic flow solutions at $\alpha = 5$ deg are shown in Fig. 9. Faster convergence is obtained with the fourth-order compact, implicit scheme of Eq. (4). Similarly, for transonic flow (Fig. 10), a faster convergence rate is obtained with the algorithm of Eq. (4). The convergence rates of the diagonal algorithms for upwind-biased schemes [Eqs. (7) and (9)] are shown next. Use of Roe or Osher Riemann solvers for the discretization of the right-hand-side convective terms does not show any difference in the convergence rate or accuracy level of the computed solution. Third-order accuracy in space is used for the evaluation of the inviscid terms as in Ref. 16. Convergence rates for inviscid flow at subsonic speeds are shown in Fig. 11; convergence rates for inviscid flow at transonic speeds are shown in Fig. 12. For both subsonic and transonic flow computations the diagonal high-order-accurate-in-space algorithms have similar convergence characteristics. These convergence rates are analogous to the rate achieved by the first-order accurate in space block-tridiagonal scheme.[16] As expected,

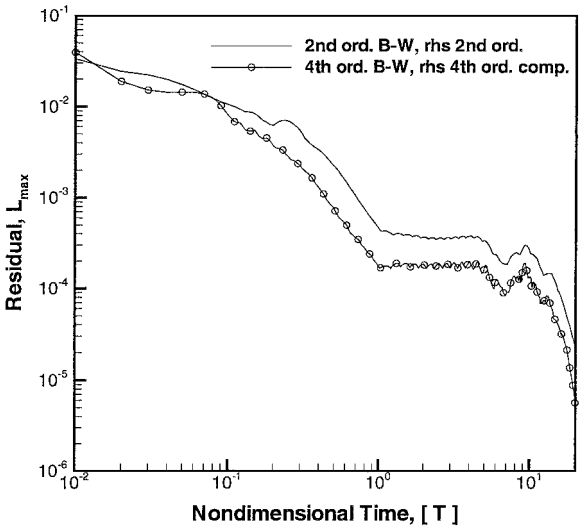

Fig. 10 Convergence rate of the diagonalized implicit algorithm (maximum residual) for inviscid flow solutions at transonic speeds; $M = 0.8$, $\alpha = 0.1$ deg, inviscid.

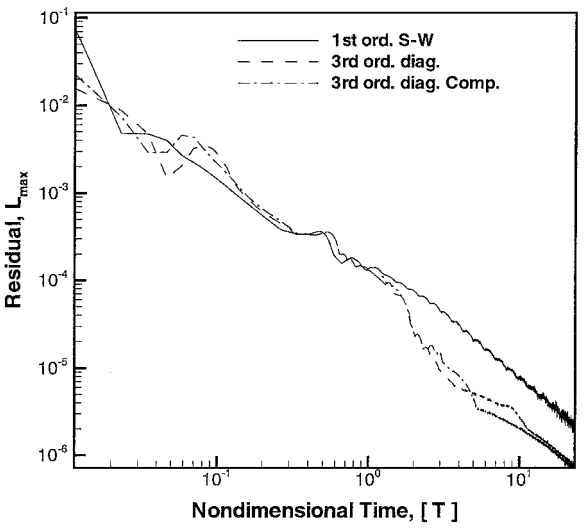

Fig. 11 Maximum residual during convergence of the block-tridiagonal and the diagonalized implicit algorithms for subsonic flow; $M = 0.3$, $\alpha = 5$ deg, inviscid.

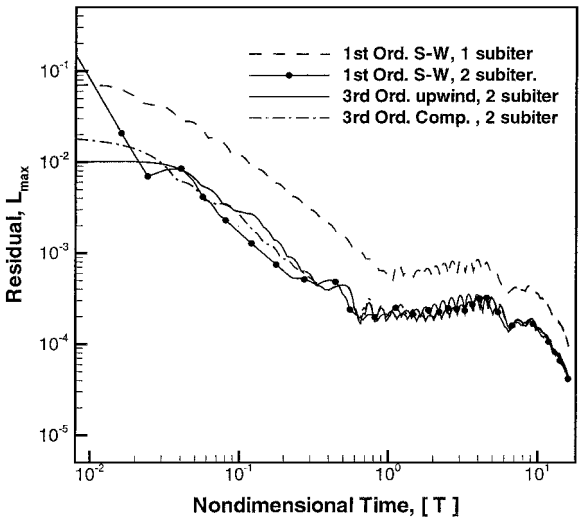

Fig. 12 Maximum residual during convergence of the block-tridiagonal and diagonalized implicit algorithms for transonic flow; $M = 0.8$, $\alpha = 0.1$ deg, inviscid.

shock capturing of steady-state solutions is not affected by the time integration method.

VII. Conclusions

High-order-accurate-in-space, implicit time integration schemes for aerodynamic applications have been developed. These schemes are based on implicit alternating direction algorithms, currently used in many CFD codes for steady-state and unsteady computations. The time accuracy of the new algorithms is still at most second order because of the linearization in time that is applied to the nonlinear fluxes. High-order-accurate implicit schemes are obtained by evaluating the spatial derivatives of the implicit operators using compact differencing schemes. As a result, the computing cost of the implicit inversion does not increase. Global high resolution is obtained when the convective terms in the right-hand-side residual terms are computed with high-order-accurate methods. The new central-difference algorithms have better convergence characteristics than their second-order accurate in space counterparts. High-order implicit ADI schemes that use explicit or compact upwind formulas to achieve a high order of accuracy in space are also shown. Algorithms that require scalar pentadiagonal matrix inversions achieve fast convergence, and they are more efficient computationally than block-tridiagonal first-order-accurate-in-space algorithms.

Acknowledgments

This research was supported by the Fluid Mechanics Division of the Army Research Office under small business innovative research (SBIR) Program Contract DAAG55-97-C-0029. Additional funding was received by NASA's SBIR Program Contract NAS2-00053.

References

[1]Abarbanel, S., and Kumar, A., "Compact High-Order Schemes for the Euler Equations," *Journal of Scientific Computing*, Vol. 3, No. 3, 1988, pp. 275–288.

[2]Adams, N. A., and Shariff, K., "A High-Resolution Hybrid Compact-ENO Scheme for Shock Turbulence Interaction Problems," *Journal of Computational Physics,* Vol. 127, No. 1, 1996, pp. 27–51.

[3]Yee, H., "Explicit and Implicit Multidimensional Compact High-Resolution Shock-Capturing Methods: Formulation," *Journal of Computational Physics,* Vol. 131, No. 1, 1997, pp. 216–232.

[4]Visbal, M. R., and Gaitonde, D. V., "High-Order-Accurate Methods for Unsteady Vortical Flows on Curvilinear Meshes," *AIAA Journal*, Vol. 37, No. 10, 1999, pp. 1231–1239.

[5]Zhong, X., "High-Order Finite Difference Schemes for Numerical Simulation of Hypersonic Boundary-Layer Transition," *Journal of Computational Physics,* Vol. 144, No. 2, 1998, pp. 662–709.

[6]Ekaterinaris, J. A., "Implicit High-Order Methods for Gasdynamics and Aeroacoustics," *Journal of Computational Physics,* Vol. 156, No. 2, 1999, pp. 272–299.

[7]de Froutos, J., and Sanz-Serna, J. M., "An Easily Implemented Fourth-Order Method for the Time Integration of Wave Problems," *Journal of Computational Physics,* Vol. 103, No. 1, 1992, pp. 160–168.

[8]Rai, M. M., and Moin, P., "Direct Numerical Simulation of Transition and Turbulence in a Spatially Evolving Boundary Layer," *Journal of Computational Physics,* Vol. 109, No. 2, 1993, pp. 169–192.

[9]Carpenter, M. H., and Kennedy, C. A., "Fourth-Order 2N-Storage Runge–Kutta Schemes," NASA TM-109112, 1994.

[10]Karniadakis, G. E., and Sherwin, S. J., "Spectral/*hp* Element Methods for CFD," *Numerical Methods in Scientific Computing*, Oxford Univ. Press, Oxford, 1999, pp. 8–14.

[11]Mavriplis, D. J., "Multigrid Strategies for Viscous Flow Solvers on Anisotropic Unstructured Meshes," *Journal Computational Physics*, Vol. 145, No. 1, 1998, pp. 141–165.

[12]Venkatakrishnan, V., and Mavriplis, D. J., "Implicit Method for the Computation of Unsteady Flows on Unstructured Grids," *Journal of Computational Physics,* Vol. 127, No. 2, 1996, pp. 380–397.

[13]Rogers, S. E., "Comparison of Implicit Schemes for the Incompressible Navier–Stokes Equations," *AIAA Journal*, Vol. 33, No. 11, 1995, pp. 2066–2072.

[14]Beam, R. M., and Warming, R. F., "An Implicit Finite-Difference Algorithm for Hyperbolic Systems in Conservation-Law Form," *Journal of Computational Physics,* Vol. 22, No. 1, 1976, pp. 87–110.

[15]Pulliam, T. H., "Artificial Dissipation Models for the Euler Equations," *AIAA Journal*, Vol. 24, No. 12, 1986, pp. 1931–1940.

[16]Ekaterinaris, J. A., and Menter, F. R., "Computation of Oscillating Airfoil Flows with One- and Two-Equation Turbulence Models," *AIAA Journal,* Vol. 32, No. 12, 1994, pp. 2359–2365.

[17]Lele, S. K., "Compact Finite Difference Schemes with Spectral-Like Resolution," *Journal of Computational Physics,* Vol. 103, No. 1, 1992, pp. 16–42.

[18]Carpenter, M. H., Gottlieb, D., and Abarbanel, S., "The Stability of Numerical Boundary Treatments of Compact High-Order Finite-Difference Schemes," *Journal of Computational Physics,* Vol. 108, No. 2, 1993, pp. 272–295.

[19]Pulliam, T. H., and Chaussee, D. S., "A Diagonal Form of an Implicit Approximate-Factorization Algorithm," *Journal of Computational Physics,* Vol. 39, No. 2, 1981, pp. 347–363.

[20]Steger, J. L., and Warming, R. F., "Flux Vector Splitting of the Inviscid Gas Dynamic Equations with Applications to Finite-Difference Methods," *Journal of Computational Physics,* Vol. 40, No. 2, 1981, pp. 263–293.

[21]Merkle, C. L., and Athavale, M., "Time-Accurate Unsteady Incompressible Flow Algorithm Based on Artificial Compressibility," AIAA Paper 87-1137, June 1987.

[22]Vichenevetsky, R., and Bowles, J. B., "Fourier Analysis of Numerical Approximations of Hyperbolic Equations," *SIAM Series in Applied Mathematics,* 1982, pp. 19–34.

[23]Ekaterinaris, J. A., "Implicit High-Order Accurate in Space Algorithms for the Navier–Stokes Equations," AIAA Paper 99-3257, June 1999.

[24]Lax, P. D., and Wendroff, B., "Systems of Conservation Laws," *Communications on Pure and Applied Mathematics,* Vol. 13, No. 1, 1960, pp. 217–237.

[25]Poinsot, T. J., and Lele, S. K., "Boundary Conditions for Direct Simulations of Compressible Viscous Flows," *Journal of Computational Physics* Vol. 101, No. 1, 1992, pp. 104–116.

[26]Harris, C. D., "Two-Dimensional Aerodynamic Characteristics of the NACA 0012 Airfoil in the Langley 8-Foot Pressure Tunnel," NASA TM-81927, April 1981.

[27]Baldwin, B. S., and Lomax, H., "Thin-Layer Approximation and Algebraic Model for Separated Turbulent Flow," AIAA Paper 78-0257, Jan. 1978.

[28]Mahesh, K., "A Family of High Order Finite Difference Schemes with Good Spectral Resolution," *Journal of Computational Physics*, Vol. 145, No. 1, 1998, pp. 332–358.

K. Kailasanath
Associate Editor